VII. ELECTRONIC TRANSPORT IN MAGNETIC MATERIALS

(1) Introduction

(2) Experimental Observations

(3) Electrical Resistivity

(4) Magnetoresistance

(1) INTRODUCTION

▶ **Electrical transport properties reflect the character of the valence electronic states in a material.**

Source of conduction electrons

• Typically *s* or *p* subshell • *f* subshell: highly localized atomic states

• *d* subshell: in between (*i.e.*, partially participate in conduction)

In metals

Transition Metals:

• *d* states connect magnetism with electrical transport properties.

• *s*-*d* hybridization causes a degree of orbital angular momentum to the conduction process.

• Empty *d* states can be occupied temporarily by conduction electrons → spin-dependent and orbital angular momentum-dependent scattering process.

In rare-earth metals and alloys:

• Conduction electrons are carried by the 5*d* and 6*s* electrons

• Magnetism: mainly from 4*f* states

• However, the conduction electrons are significantly polarized by exchange with *f* states, and thus magnetism affects transport in these metals and alloys

In Oxides

• Thermally activated electrons from *s*-*d* or *p*-*d* bonds

• The spin of the valence states are intimately connected with magnetism by exchange and crystal field interactions.

• Magnetism is connected with electrical transport processes.

(2) Experimental Observations

(i) Temperature dependence of resistivity $\rho(T)$ in Metals (see Fig 15.1 in O'handley)

- Nonmagnetic metals: $\rho(T) = \rho_0 + \alpha T$ (above Debye temperature)
- Ferromagnet: an anomaly near a magnetic transition
- When spins are disordered (Ni above T_c and Pd over all temperatures), an electron is more likely to scatter than if it moved in a medium of uniform magnetization (Ni below T_c)
- High ρ of the paramagnetic state is attributed to electron scattering from the disorder in the spin system in addition to that from lattice vibrations.

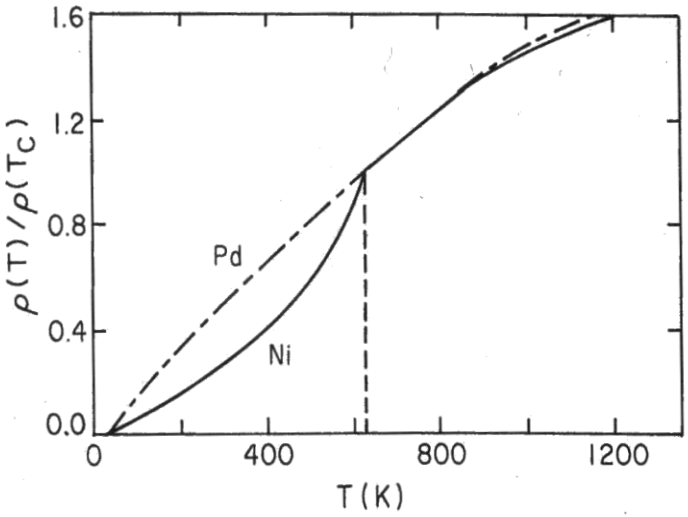

Figure 15.1 Resistivities of Ni and Pd normalized to their values at T_c of Ni, 631 K, versus temperature. [After Gerritsen (1956).]

(2) Experimental Observations

(ii) $\rho(T)$ in Oxides

- Conductivity $\sigma \propto \sigma_0 \exp[-2E_g/k_BT]$, where E_g: the energy gap between the occupied valence states and the empty (at 0 K) conduction states.
- CMR materials : $La_{1-x}Ca_xMnO_3$ (see Fig. 15.2 in O'handley)

Metal-semiconducting transition at a temperature where a weak magnetic moment still exists.

The peak of the field-induced resistance change, $\triangle R/R(H)$, is shifted to lower temperature by ~25 K compared to the metal-semiconducting transition.

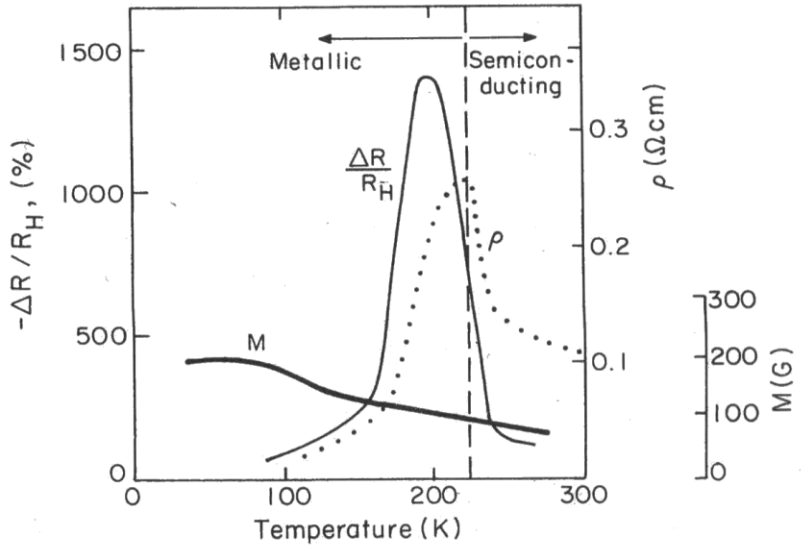

Figure 15.2 Variation of MRR, resistivity, and magnetization in laser-deposited $(La_{2/3}Ca_{1/3})MnO_3$ films. [After Jin *et al.* (1994).]

(2) Experimental Observations

(iii) ρ due to Dilute Magnetic Impurities

Addition of transition metal impurities to noble metal hosts

$\rho(x) = \rho(0) + (d\rho/dx)x$

where, $\rho(0)$ = resistivity of a pure noble metal host

x = the impurity concentration in $Cu_{1-x}\,X_x$

The slope $d\rho/dx$ of for transition metal impurities in Cu

(see Fig 15.3 in O'handley)

- A splitting in energy of the impurity $3d(\uparrow)$ and $3d(\downarrow)$ states
- If these states coincide with the conduction band Fermi level, there is enhanced scattering of charge carriers into these states, leading to increase in resistivity.
- Conduction electron scattering with localized d states depends on
  (1) the relative spin of the two electronic states involved and
  (2) the relative number of initial and final states for scattering, specially, the density of $3d$ spin up and down states.

→ the density of magnetic states at E_F is important in addition to spin ordering in ρ of ferromagnetic metals.

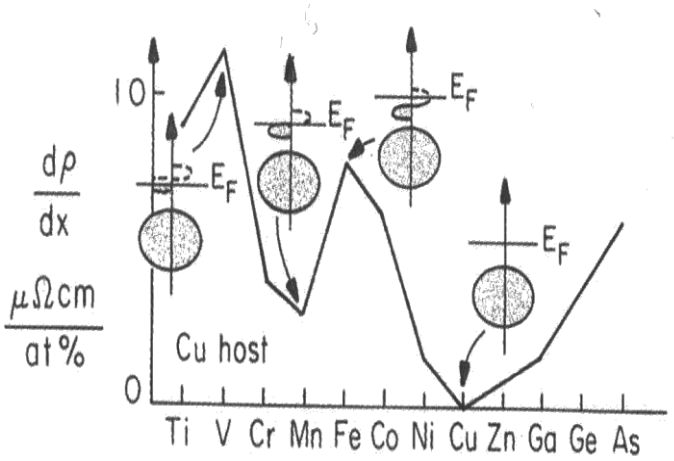

Figure 15.3 Variation with impurity type for the slope $d\rho/dx$ of Cu with transition metal impurities in Cu: $Cu_{1-x}X_x$. [Adapted from Kittel (1963).]

(3) Electrical Resistivity

Low temperature electrical resistivity values and the shape of the density of states in various metals

(see Fig. 15.4 in O'handley)

For *free* electrons,

Simple Drude model

$1/\rho = \sigma = ne^2\tau/m^*$

where n = concentration of free carriers

τ = relaxation time

m^* = effective mass of the charge carriers

applicable only to *s*-electron metals

(not to metals of *d* band-intersection with E_F)

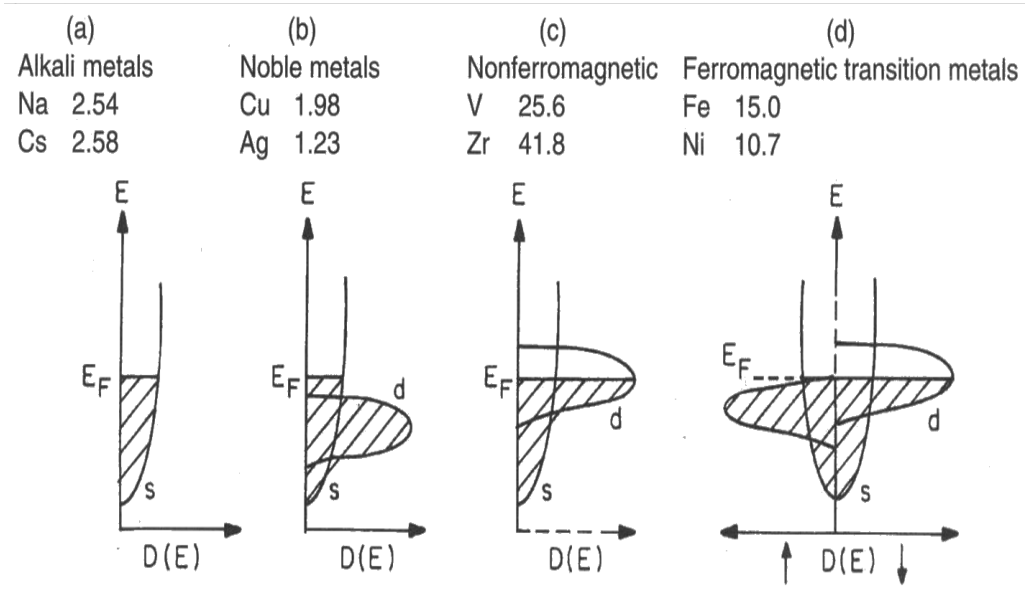

Figure 15.4 Examples of electrical resistivity at the Debye temperature (ρ in $\mu\Omega\cdot$cm) for four classes of metals (below, schematic state densities for each class: (*a*) alkali metals; (*b*) noble metals; (*c*) nonferromagnetic transition metals; (*d*) ferromagnetic transition metals.

How does the presence of *d*-states near E_F affect charge transport properties?

(i) Hybridization of *s* and *d* states makes free electron concentration small.

(ii) When s and d states hybridize, effective mass m^* increases and thus the mobility μ ($= e\tau/m^*$) is reduced.

(iii) Free electrons get scattered into more localized *d* states and thus decreases the relaxation time, and the mobility is further suppressed.

(3) Electrical Resistivity

What are the differences between ferromagnetic and nonferromagnetic transition metals?

(i) The spin direction of the charge carriers is conserved during most scattering events at temperatures well below T_c (first by Mott, 1936 yr).

(ii) The charge carriers having spin up and spin down can be represented as two parallel paths: **Two-current Model for Transition Metals** (see Fig. 15.5 in O'handley)

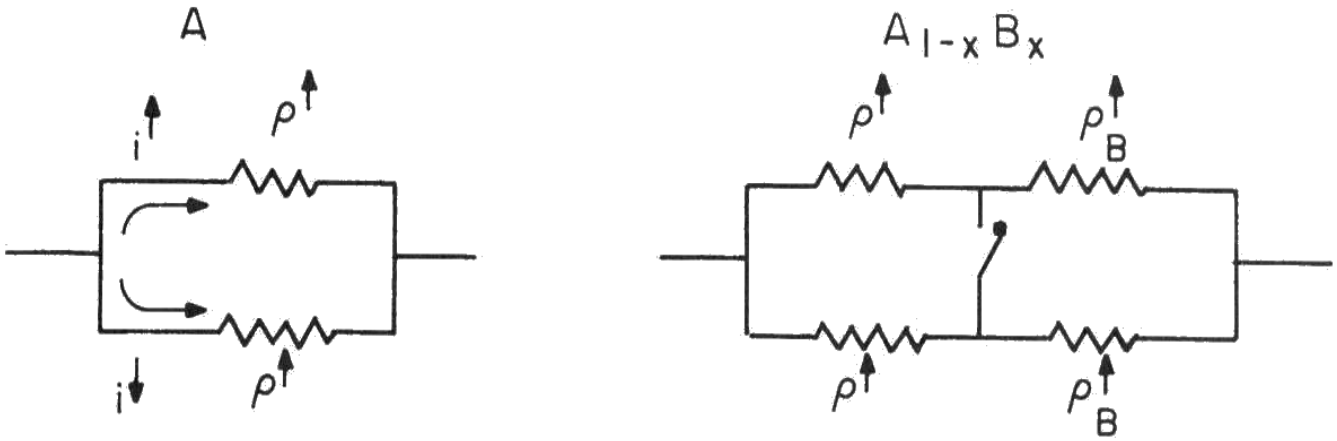

Fig 15.5 Equivalent circuits for the two-current model of resistivity in pure transition metals(left) and dilute transition metal alloys(right)

(3) Electrical Resistivity

Scattering sources in a single element conductor: phonon, impurity, *s-d* hybridization and others

At low temp ($T < T_c$)

$$\rho = \rho^{\uparrow}\,\rho^{\downarrow}/(\rho^{\uparrow} + \rho^{\downarrow}),\quad \alpha = \rho^{\downarrow}/\rho^{\uparrow}$$

For Ni, Co and many strongly magnetic alloys, $\alpha << 1$

Impurities or alloying elements (B in $A_{1-x}B_x$)

- Without spin mixing (T < Tc):

  similar to the above expression.

$$\frac{\Delta\rho(H)}{\rho_{av}} = \frac{\Delta\rho}{\rho_{av}}\left(\cos^2\theta - \frac{1}{3}\right)$$

- If spin mixing(or spin-flip scattering) (T > Tc):

  lower resistivity

$$E = \rho J$$

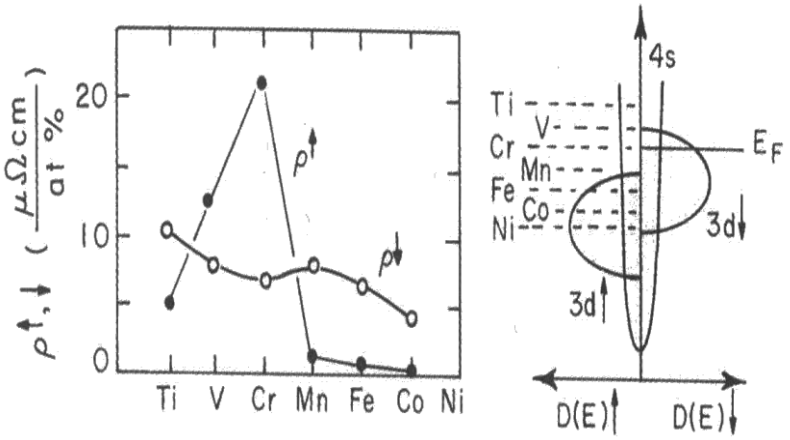

Figure 15.6 Left, resistivities determined for the spin-up and spin-down impurity bands determined from measurements on Ni host (Campbell and Fert 1982). Illustration at right shows a schematic of the band structure of the Ni host with the centroid of the majority-spin *d*-states of the impurities indicated.

- 3*d* impurities in Ni (see Fig. 15.6 in O'handley)
- If the energy of the majority-spin 3d↑impurity states are close to the Ni Fermi level, $\rho^{\uparrow}$ increases like Cr and V.

(3) Electrical Resistivity

Temperature Dependence (see Fig.15.7 in O'handley)

Two contributing effects

(1) Conduction electron spin scattering

from disorder in *M*

$$\rho_{ferro} = \rho_{para}\frac{(J-|<J>|)(J+1+|<J>|)}{J(J+1)} \approx \rho_{para}[1-(\frac{M_s(T)}{M_s(0)})^2]$$

Origin: exchange interaction between

the spin of the charge carrier *s* and

the local, paramagnetic

(or disordered ferromgnetic) moment

(2) Magnon creation or annihilation at T > Tc

$$\rho_{highT} = \frac{\rho\uparrow\rho\downarrow+\rho\uparrow\downarrow(\rho\uparrow+\rho\downarrow)}{\rho\uparrow+\rho\downarrow+4\rho\uparrow\downarrow}$$

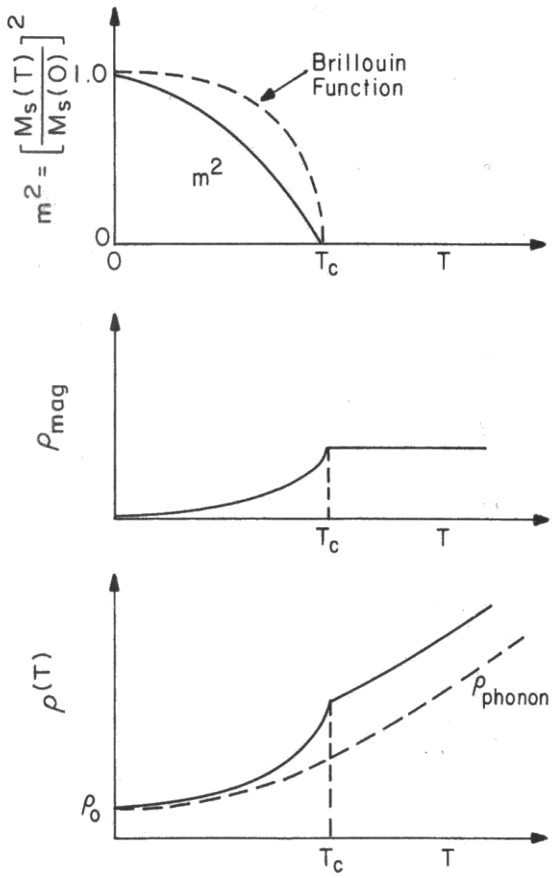

Figure 15.7 Above, temperature dependence of reduced magnetization squared. Center, temperature dependence of spin disorder scattering that goes as $1\text{-}m^2(T)$. Below, addition of spin disorder resistivity to the residual and phonon contributions to electrical resistivity.

(4) Magnetoresistance (Galvanomagnetic Effects)

Nonmagnetic Materials (see Fig.15.8 in O'handley)

▶ **Ordinary Hall Effect**

- E_H**(a transverse electric field) =** $R_H(J \times \mu_0 H)$
- Origin: Lorentz force ($F = q(v \times H)$) on the current carriers, leading to cyclotron orbits.
  - $J_y = ne\langle v_y \rangle$**, thus** $R_H = 1/ne$
  - **Hall resistivity** $\rho_H = E_H/J_x = R_H \mu_0 H$

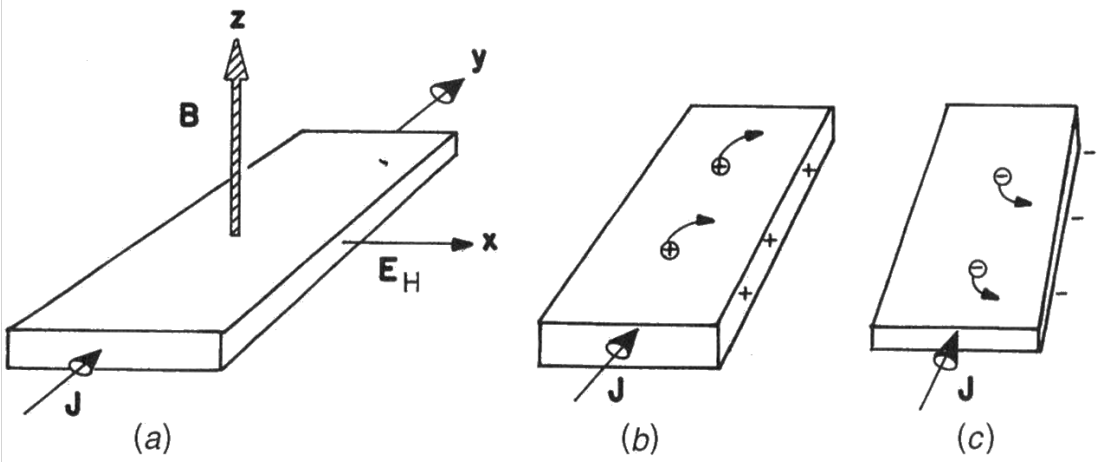

▶ **Magnetoresistance**

- **Kohler's rule:** $\Delta\rho/\rho = f(H/\rho)$
- Because a deflection of a charge carrier in either direction away from J_x increases, the change in resistance must be an even power of H.
  - **MR ratio** $\Delta\rho/\rho \propto (H/\rho)^2 \leftrightarrow \rho_H \propto H$

(4) Magnetoresistance

Magnetic sensors (see Fig.14.19 in J. M. D. Coey)

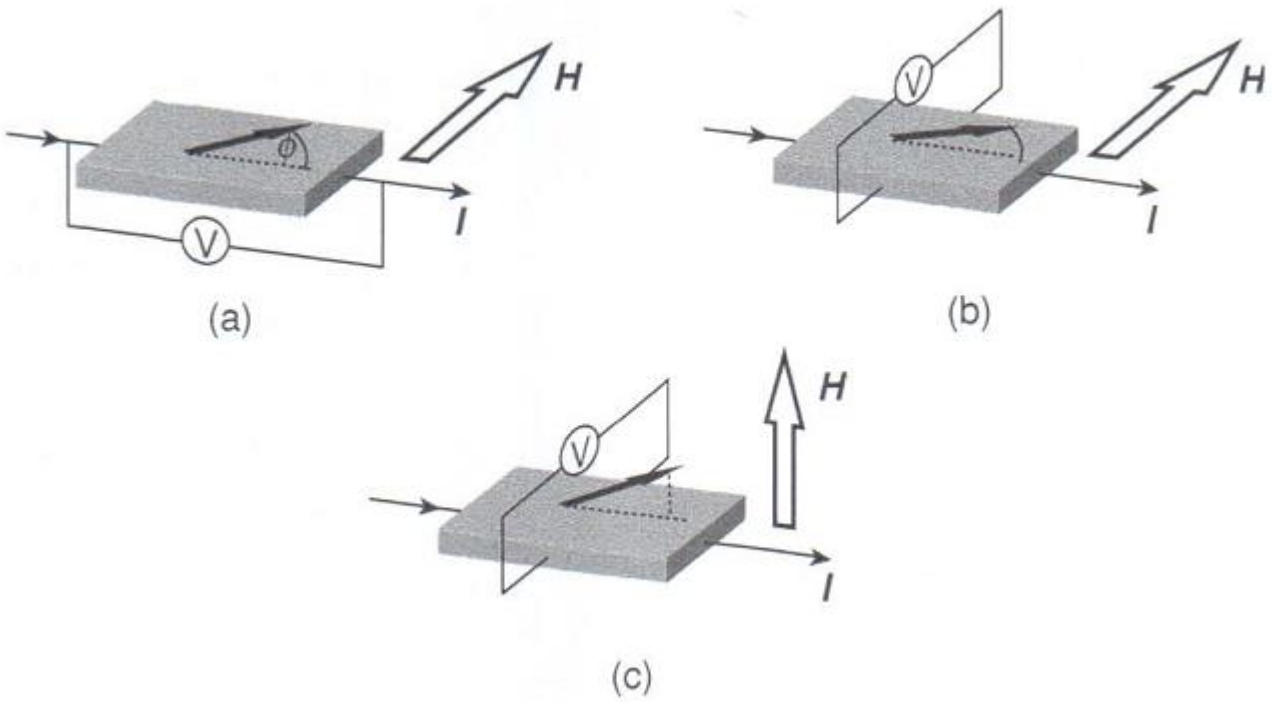

Fig. 14.19 (a) AMR, (b) planar Hall and (c) anomalous Hall effect sensor configurations. The easy direction is shown by the dashed line.

(4) Magnetoresistance (Galvanomagnetic Effects)

Ferromagnetic Materials (see Fig.15.10 in O'handley)

▶ **Anomalous(extraordinary, spontaneous) Hall Effect (greater strength relative to ordinary Hall effect)**

• The microscopic internal field associated with M couples to the current density in ferromagnets is the spin-orbit interaction between the electron trajectory (orbit) and the magnetization (spin).

• $\rho_H = E_H/J = \rho_{oH} + \rho_{sH}$
$= \mu_0(R_0 H + R_s M)$

• Anomalous (or spontaneous) Hall effect is observed at low field : ρ_{sH}

• Ordinary Hall effect is observed at high field : ρ_{oH}

From the figure

ρ_{sH} = the value of the high-field Hall resistivity extrapolated to B=0
- Dramatic increase with increasing *x, why?*

ρ_{oH} = high-field slope
- Unaffected by the Al impurities (R_0 <0 : conduction by electrons)

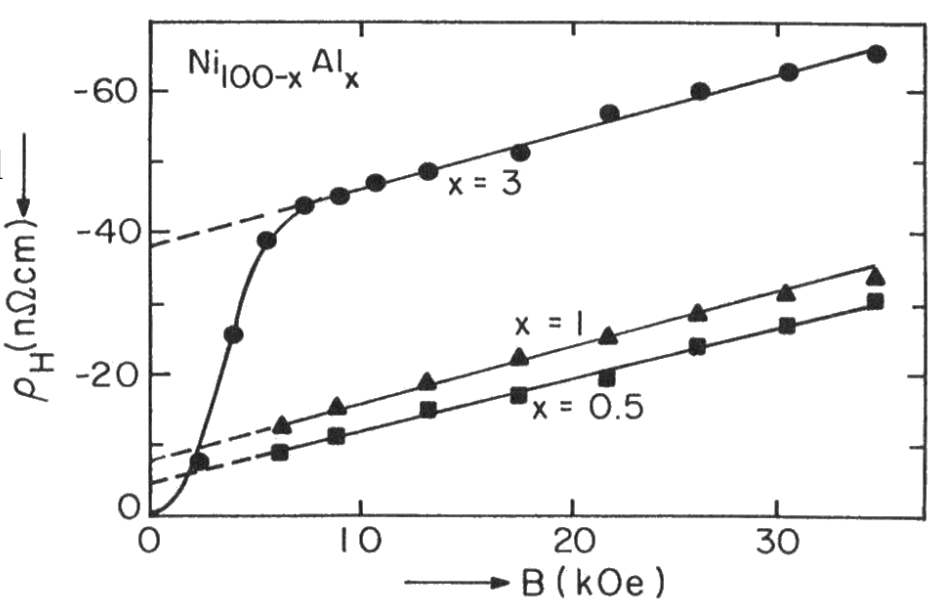

fig. 15.10 Field dependence of Hall resistivity in Ni on Al impurity content

(4) Magnetoresistance (Galvanomagnetic Effects)

Ferromagnetic Materials

▶ Anomalous(extraordinary, spontaneous) Hall Effect (continued)

Temperature dependence of the magnetization and spontaneous Hall resistivity in amorphous $Gd_{17}Co_{83}$

- Below a certain temperature (called, compensation temperature), the sign of Hall resistivity reverse its sign:
  below this temp → Gd moments are dominant,
  above this temp → Co moments are dominant.

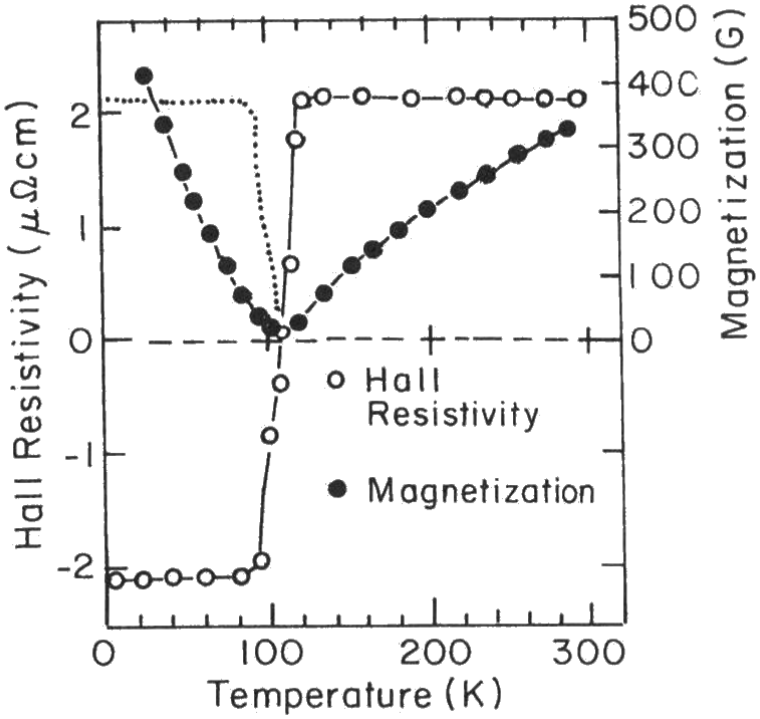

Fig 15.13 Temperature dependence of the magnetization and spontaneous Hall resistivity in Gd17Co83

(4) Magnetoresistance (Galvanomagnetic Effects)

Ferromagnetic Materials

▶ **Anisotropic Magnetoresistance (AMR)**

• Kohler's rule for a ferromagnet

$\Delta\rho/\rho \propto a(H/\rho)^2 + b(M/\rho)^2$

→ spontaneous(or anisotropic) MR

AMR effect

$\Delta\rho(H)/\rho_{av} = (\Delta\rho/\rho_{av})(\cos^2\theta - 1/3)$,

θ = angle between J and M

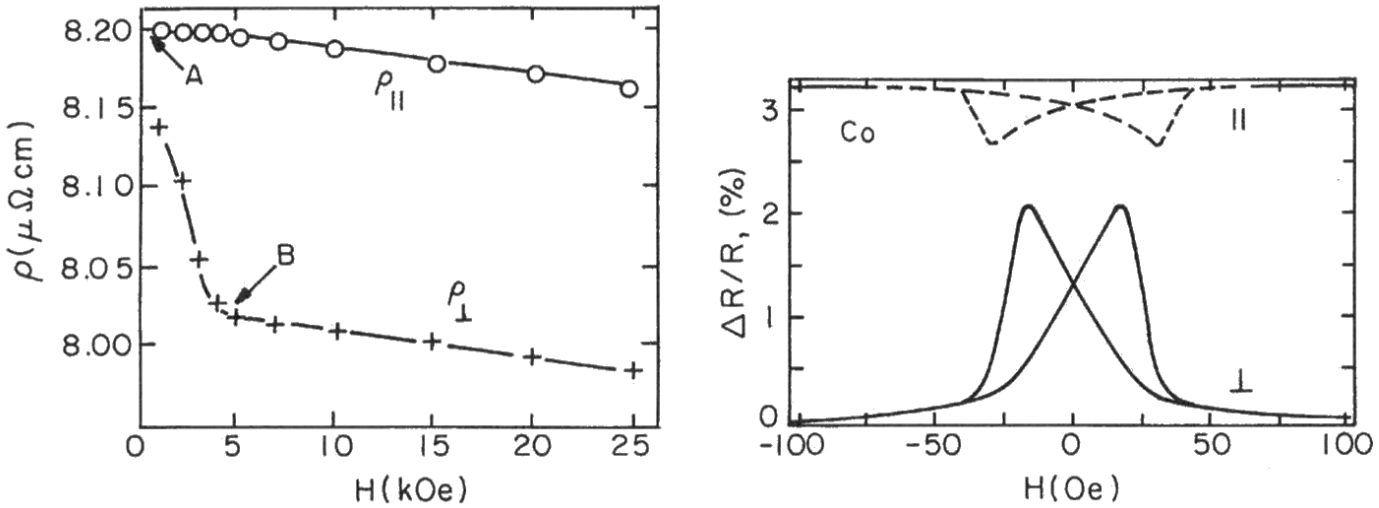

Fig 15.14 (a)Resistivity of Ni0.9942Co0.0058 at room temperature versus applied field (McGuire 1975); (b) low-field magnetoresistance for cobalt thin film showing even field symmetry and hysteresis [After Parkin (1994)]

(4) Magnetoresistance (Galvanomagnetic Effects)

Ferromagnetic Materials

▶ Anisotropic Magnetoresistance (AMR) (continued)

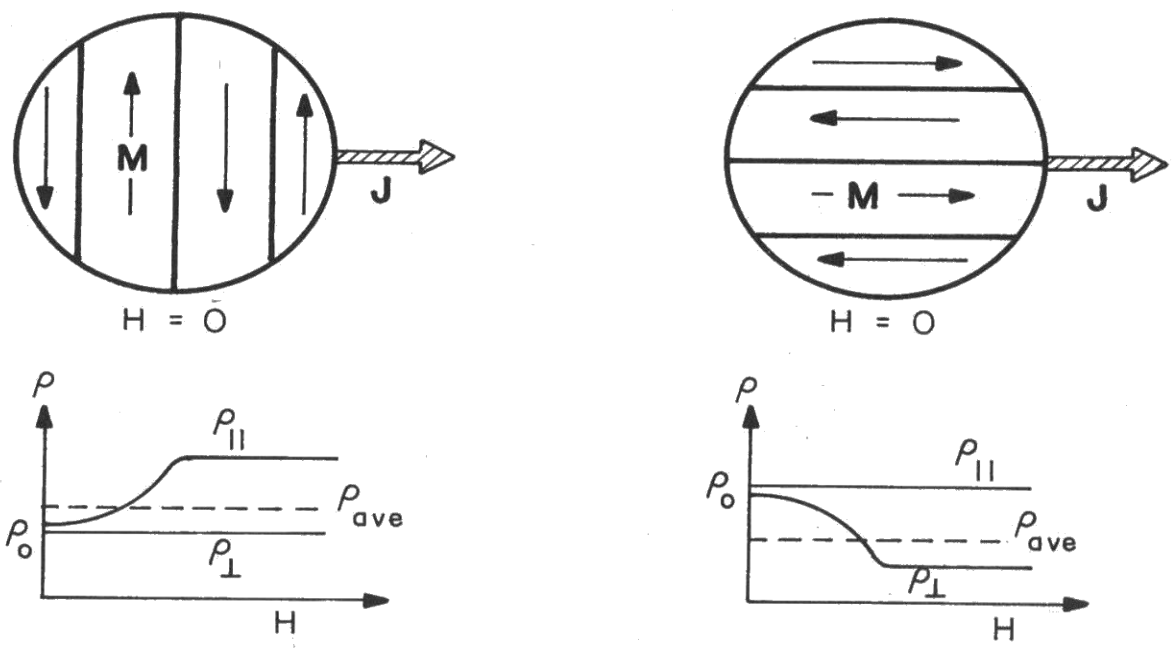

Figure 15.15 Field dependence of resistivity in fields parallel and perpendicular to J reveals the extraordinary or anisotropic magnetoresistance effect $\Delta\rho = \rho_{||} - \rho_{\perp}$ at low fields superimposed on the ordinary effects (quadratic in H) at higher fields. Note that in zero field, the resistance may be larger or smaller than ρ_{av} depending on the equilibrium domain structure. (Compare with Fig. 7.5 for magnetostriction.)

(4) Magnetoresistance (Galvanomagnetic Effects)

Ferromagnetic Materials

▶ Anisotropic Magnetoresistance (AMR) (continued)

Composition dependence of AMR (see Fig. 15.16)

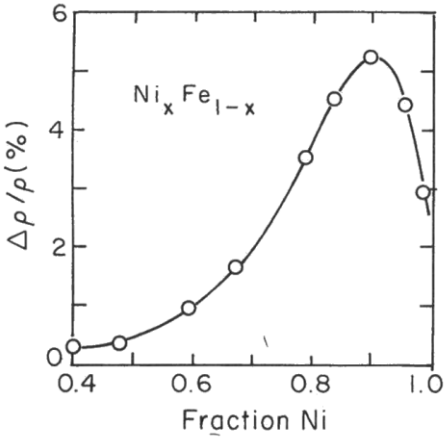

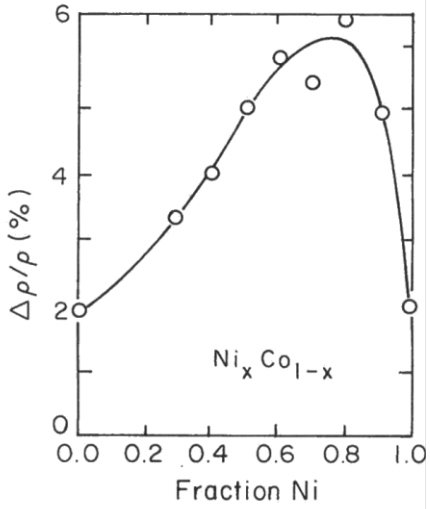

AMR ratio versus avg. Bohr magnetron (see Fig. 15.17)

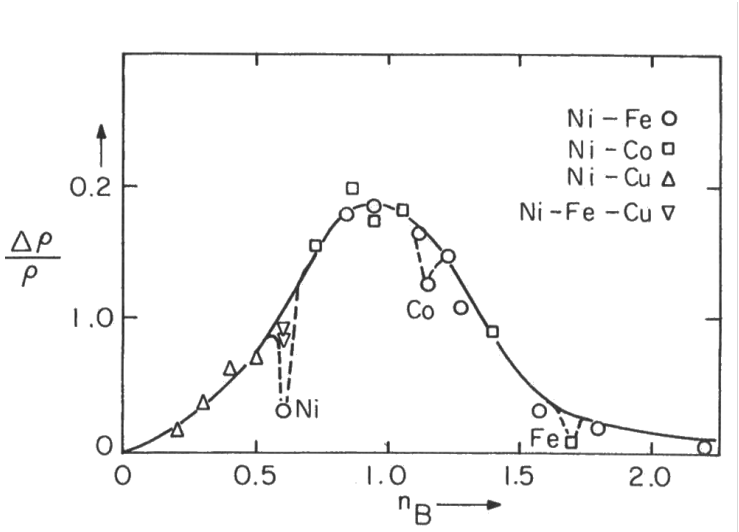

(4) Magnetoresistance

Ferromagnetic Materials

▶ Giant Magnetoresistance (GMR)

Definition of GMR ratio

(1) The change in resistance ΔR to its high-field value

(2) The change in resistance ΔR to its low-field value

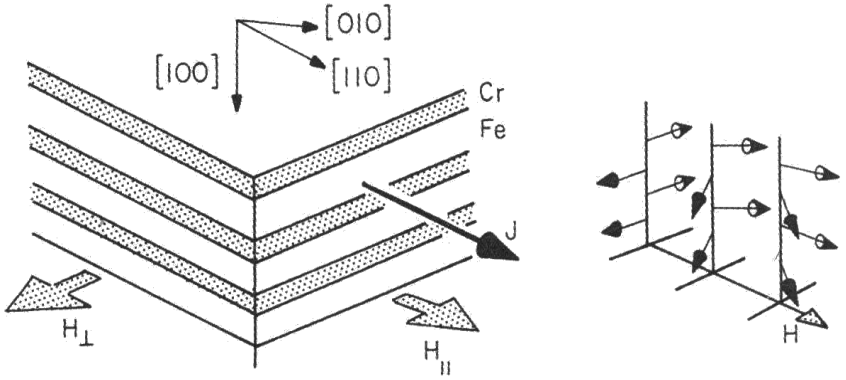

Fig 15.22 Left: relative orientation of Fe easy axes, current(J) and applied field (H) Right: Schematic of magnetization process with increasing H. Magnetocrystalline anisotropy has been ignored.

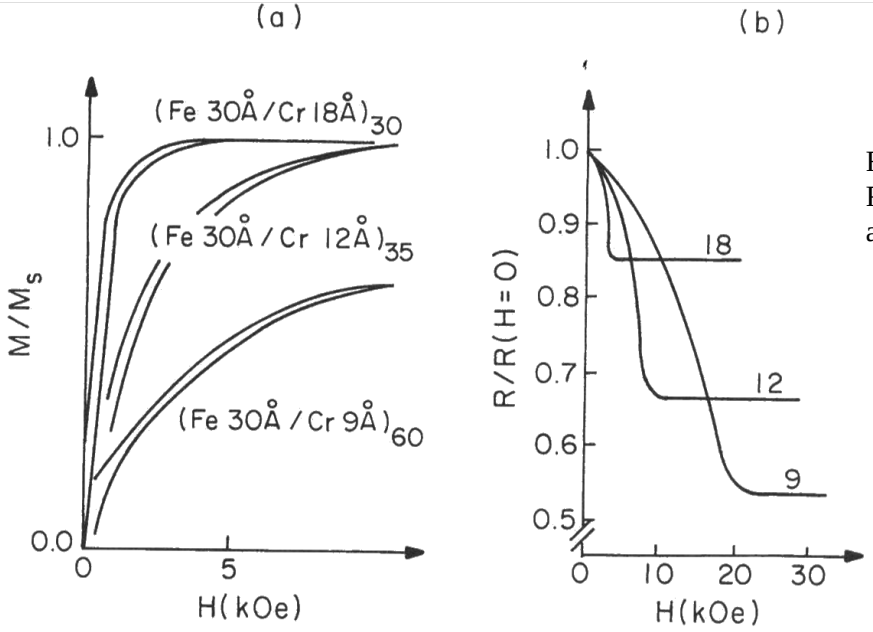

Fig 15.23 (a) Hysteresis loop for three different Fe-Cr multilayers at 4.2 K (b) Relative change in R with H//J at 4.2 K

- **Antiferromagnetically coupled → difficult to saturate**
  (Saturation field of 20 kOe)
- **The strength of AF coupling depends on the Cr layer thickness**
- **Resistivity becomes larger with decreasing Ha (*i.e.*, less aligned moments)**
- **Dependence of ρ on M_1(Fe) and M_2(Cr) becomes more significant when the AF coupling is stronger (0.9 nm Cr) (*i.e.*, when the moments of adjacent layers in zero field are almost completely antiparallel)**
- **Sometimes, $\Delta R/R = (R_{AF} \; R_F)/R_F$ since not always complete *AF* coupling (*i.e.*, $M = 0$) when Ha = 0**

(4) Magnetoresistance

Ferromagnetic Materials

▶ **Giant Magnetoresistance (GMR)**
Fe-Cr multilayers (continued)

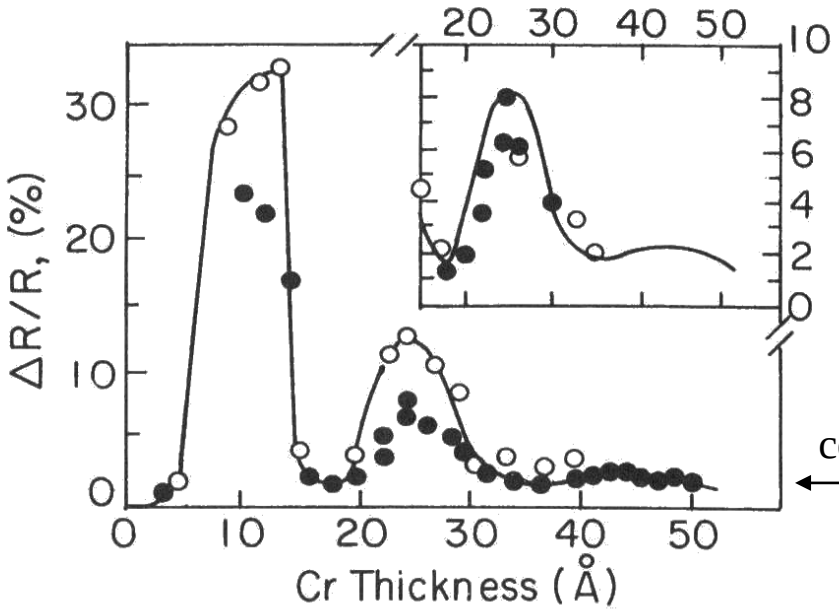

Fig 15.24 Transverse saturation MR at 4.2 K versus Cr layer thickness : N = 30 (closed circles) deposited at 40°C , N =20 (open circles) deposited at 125°C

- Oscillatory exchange coupling
- With increasing the thickness of the Cr layer, the oscillations in magnitude of the field needed to saturate the magnetization and in the magnitude of the MR ratio are observed to be in phase.
- The MR maxima occur at Cr layer thickness for which the magnetic layers are coupled antiferromagnetically: 2 maxima in AF coupling (also in GMR ratio) occur at spacer (Cr) thickness of 9 and 24 Å for Fe/Cr, 8 and 19 for Co/Cu multilayers
- At least 4 oscillations in MR at the temp range from 1 to 400K

compare!!

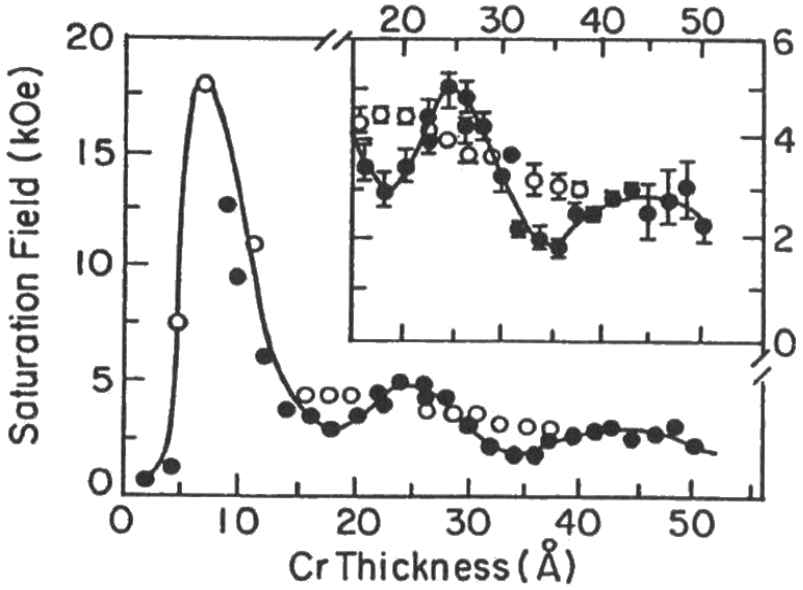

(4) Magnetoresistance

Ferromagnetic Materials

▶ Giant Magnetoresistance (GMR) (continued)

The GMR ratio in multilayer systems

- Not a function of the angle between J and M as it is for AMR, but dependent on the relative orientation of M in adjacent layers.
→ mechanism is different from AMR effect.

- According to Dieny *et al.*

$$\triangle\rho(\varphi)/\rho = (\triangle\rho/\rho)_{GMR}\,(1\cos\varphi)/2$$

where φ = angle between $\boldsymbol{M}_1$ and $\boldsymbol{M}_2$ in the two sets of layers

In Fig. 15.22, θ ($\angle$ between $\boldsymbol{M}$ and $\boldsymbol{H}$) = $\varphi/2$

$$\triangle\rho(\theta)/\rho = (\triangle\rho/\rho)_{GMR}\,(1\cos 2\theta)/2$$

$$= (\triangle\rho/\rho)_{GMR}\,\sin^2\theta$$

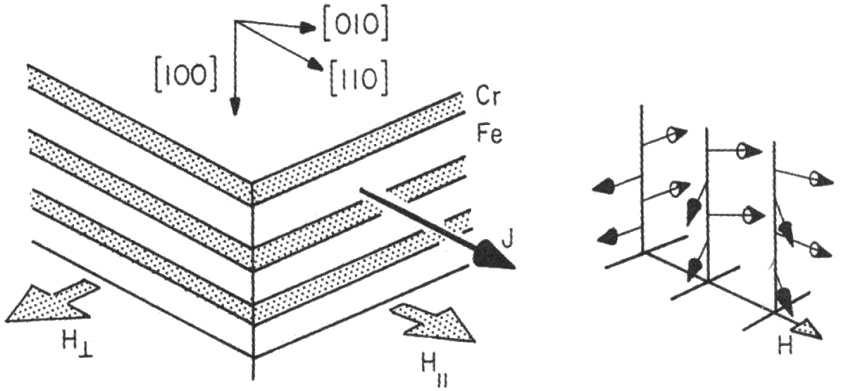

Fig 15.22 Left, relative orientation of iron easy axes, current and field for ReCr multilayers [after Baibich et al. (1988]; right, schematic of magnetization process in the multilayers with increasing field strength. Magnetocrystalline anisotropy has been ignored.

- For hard axis magnetization, approximate form of the field dependence observed for GMR in antiferromagnetically coupled multilayers:

Since $M/M_s = \cos\theta = H/H_a$

Therefore, $\triangle\rho(\theta)/\rho = (\triangle\rho/\rho)_{GMR}[1 - (H/H_a)^2]$

(4) Magnetoresistance

Ferromagnetic Materials

▶ Giant Magnetoresistance (GMR) (continued)

Source of scattering

- Experimental data support that *scattering occurs at the interfaces of layers* (see the figures).

- While exchange coupling is only weakly dependent on temperature, the GMR ratio at low temp is much larger than that of room temperature. (~ 4 times)

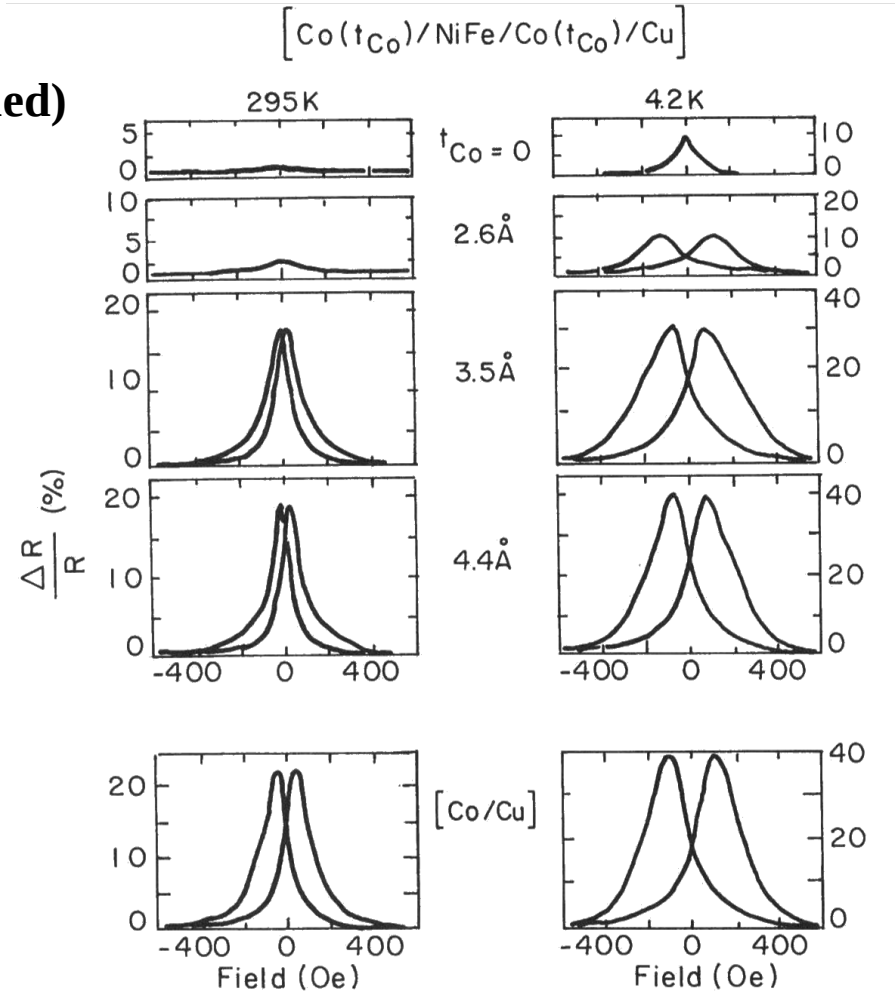

Fig 15.25 GMR ratio versus H for various Co thickness in FeNi multilayers and for [Co/Cu] multilayers at 295 K (room temp.) and 4.2 K

(4) Magnetoresistance

Ferromagnetic Materials

▶ **Giant Magnetoresistance (GMR) (continued)**

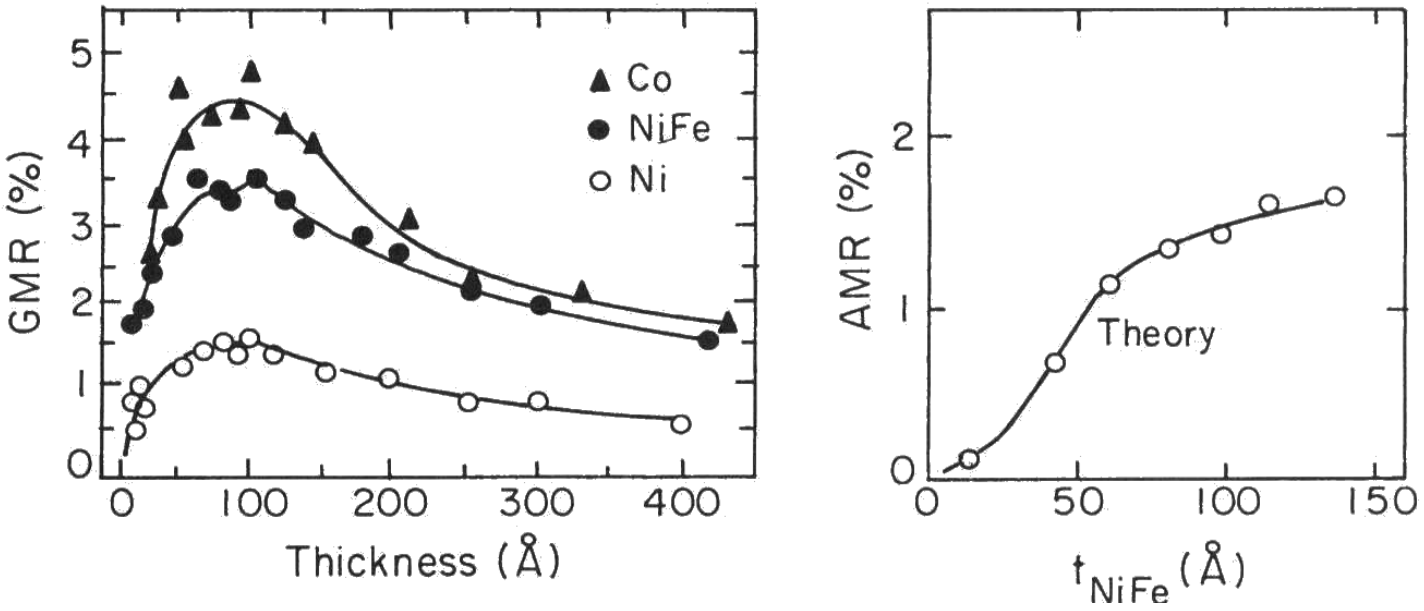

Fig 15.26 Left : Variation of GMR with magnetic layer thickness in various GMR spin valve structures. Right : MR versus NiFe thickness

(4) Magnetoresistance

Ferromagnetic Materials

▶ Giant Magnetoresistance (GMR) (continued) : Mechanism of GMR

Observations:

- GMR depends on the relative orientation of the magnetization in adjacent magnetic layers.
- GMR effects disappears if the spacer layer thickness become much larger than the mean free path of the electrons (of the order of 10 nm)

Important scattering events:

- Dependent on the relative spin of the carrier and the scattering site → spin-orbit scattering is less important for GMR.
- Spin-spin scattering between the spins of charge carrier and the scattering site, respectively

Phenomenological model

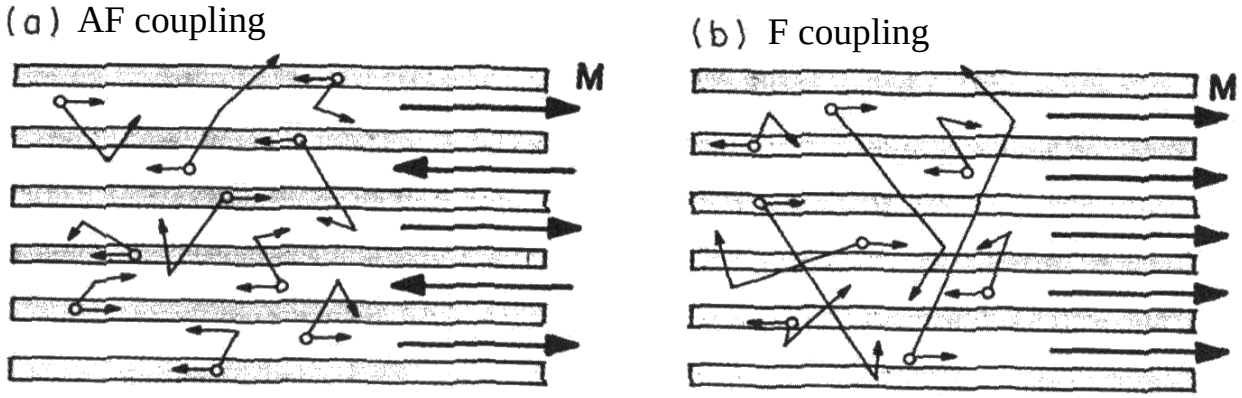

Fig 15.27 Charge carriers of majority and minority spin are shown as well as hypothetical trajectories with different scattering lengths. In F case, the charge carriers with spin parallel to the direction of magnetization has a longer mean free path.

(4) Magnetoresistance

Ferromagnetic Materials

▶ Giant Magnetoresistance (GMR) (continued) : Mechanism of GMR

Equivalent circuits for multilayers : Two-current model (Assuming spin-dependent scattering is more likely when a carrier of one spin encounters a scattering site of opposite spin.)

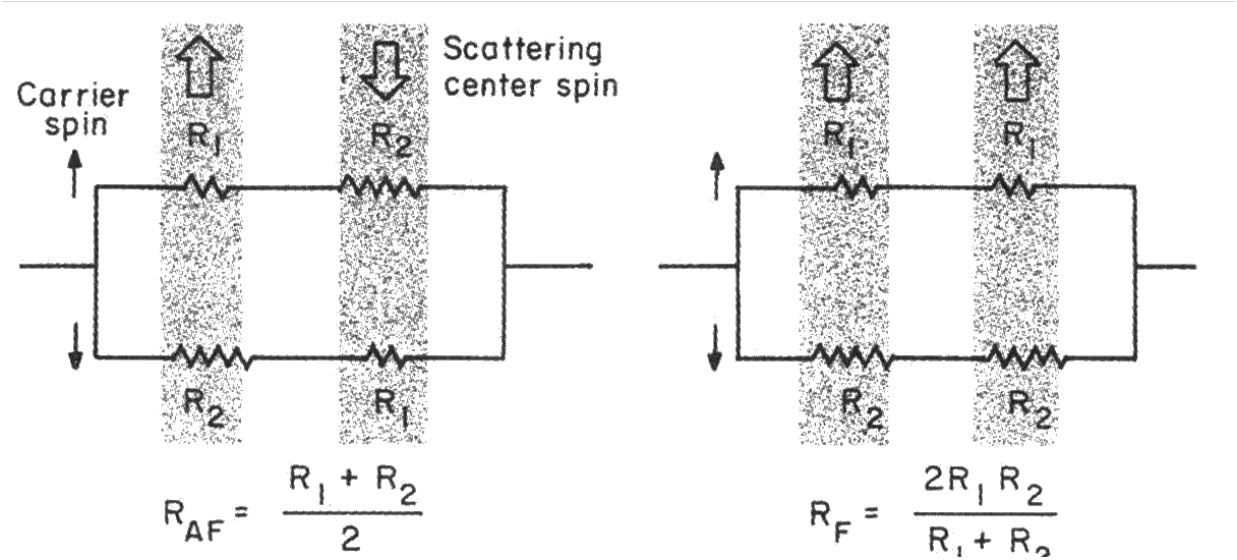

Fig 15.28 - Upper path: the resistance due to spin-dependent scattering of upward-spin electrons
- Lower path: that of downward-spin electrons
- Shaded regions: Magnetic layers with their direction of magnetization indicated by the open arrow.
- R_1: like-spin scattering, R_2: unlike-spin scattering
(Spin -independent scattering in the spacer layer is omitted.)

(4) Magnetoresistance

Ferromagnetic Materials

▶ **Giant Magnetoresistance (GMR) (continued) :**

Two-current Model

[A] Current in-plane (CIP) geometry

(1) In antiferromagnetically coupled multilayers,

Conduction electrons of either spin having sufficiently long mean free paths will thermally sample a series of strong and weak scattering layers as they draft about the electric field direction from one magnetic layer to another. Thus carriers of either spin direction have comparable mean free paths and resistivities.

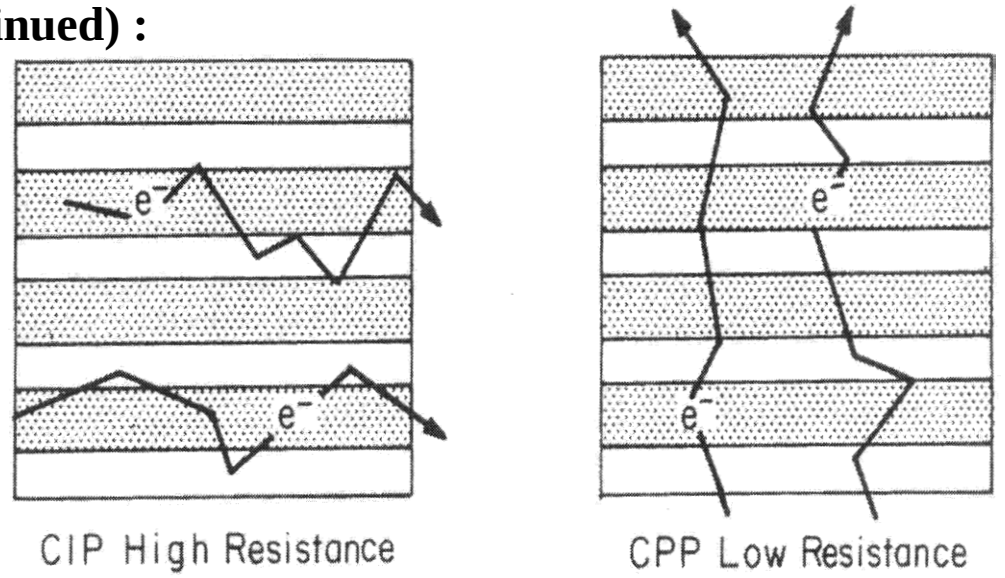

Fig 15.31 Schematic illustrations of CIP and CPP GMR geometries. In both cases the film's thickness is vertical and its lateral extent is truncated in the drawing

(2) In ferromagnetically coupled multilayers

Carriers of the same spin direction as that of the magnetic layers will sample a series of weakly scattering, parallel-spin layers. Hence, their mean free path is longer and their resistivity smaller compared to those of carriers having spin opposite that of the magnetic layers.

[B] Current perpendicular to plane (CPP) geometry

Advantage: Electron are forced to transverse many interfaces, leading to very large GMR effect

Disadvantage: R is extremely small normal to its plane, making measurements difficult.

(4) Magnetoresistance

Magnetic Oxides

▶ Colossal Magnetoresistance (CMR) :

- Large MR duet to phase transformation: insulator ↔ metal
- 1st report by R. Von Helmolt *et al*., Phys. Rev. Lett. 71 (1993) 2331
- named, "CMR" by S. Jin et al., Science, 264(1994) 413
- Parent compounds: $LaMnO_3$

  In general, $T_{1-x}D_xMnO_3$, x = 0.2 ~ 0.4 (hole doping)

  where, T (trivalent lanthanides) : La, Nd, ...

  D (divalent alkaline earths) : Ca, Sr, Ba
- advantage: very large MR values (> 100,000%)
- disadvantage: large magnetic field (5T) required for obtaining a significant MR values

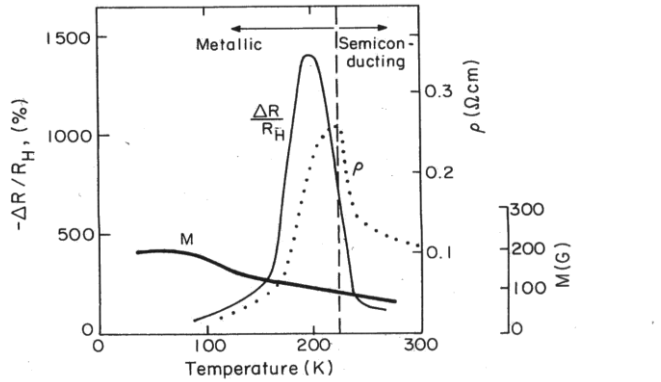

Figure 15.2 Variation of MRR, resistivity, and magnetization in laser-deposited $(La_{2/3}Ca_{1/3})MnO_3$ films. [After Jin *et al.* (1994).]

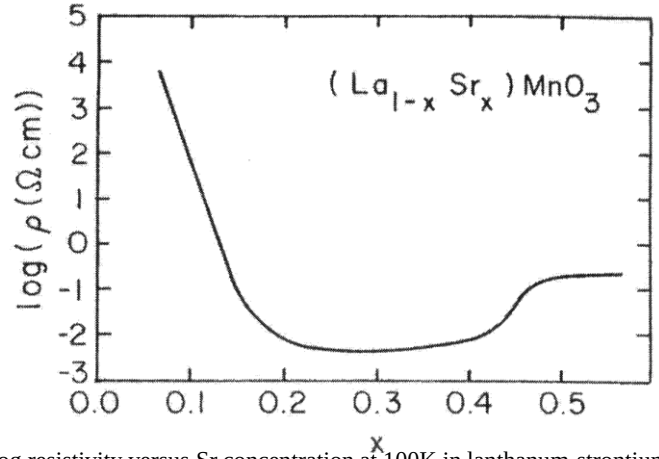

Fig 15.45 Log resistivity versus Sr concentration at 100K in lanthanum-strontium manganate (Jonker and Van Santen 1950). The six orders of magnitude drop in resistivity near x=0.1 corresponds to the insulator-to-metal transition.

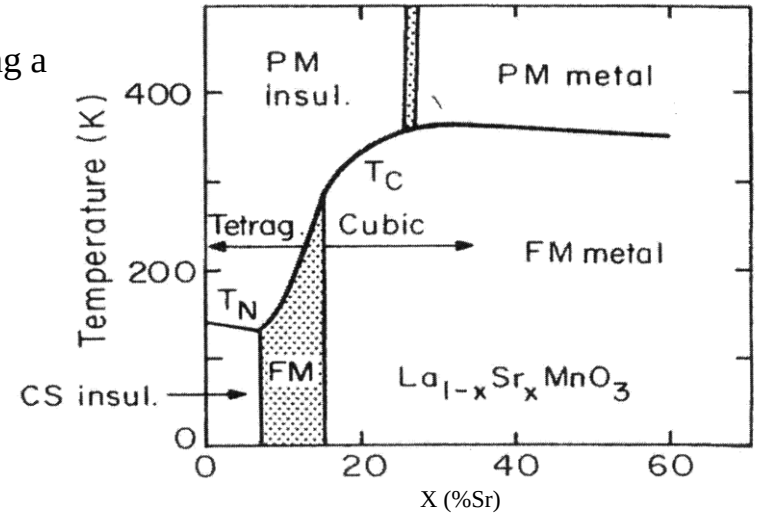

Fig 15.46 Magnetic phase diagram of $La_{1-x}Sr_xMnO_3$. PM is paramagnetic and FM is ferromagnetic. The drop in resistivity near x=0.1 in figure 15.45 corresponds here to the transition from a canted spin (CS) insulator to a ferromagnetic metal at 100K

(4) Magnetoresistance

Ferromagnetic Materials

▶ Applications

Spin Valves (coined by Dieny *et al*., 1991): Application of the GMR effect.

- Two magnetic layers (one is magnetically soft, the other is magnetically hard or pinned.) separated by a nonmagnetic conductor are uncoupled or weakly coupled in contrast to the generally strong AF exchange operating in Fe-Cr-like multilayer systems

→ Thus MR change can be made in fields of a few tens of Oe since the angle of the moments of these two magnetic layers can be changed at a modest field.

Operation of the spin valve

Two different exchange couplings

- Stronger exchange coupling of the pinned layer to the AF FeMn layer.
  A function of K_u of the AF and the interfacial coupling energy of F-AF

- Weaker exchange coupling between the two F layers through the interfacial coupling energy of F-F balanced by antiparallel dipole coupling

Applications of spin valve

Field sensors, Transistors

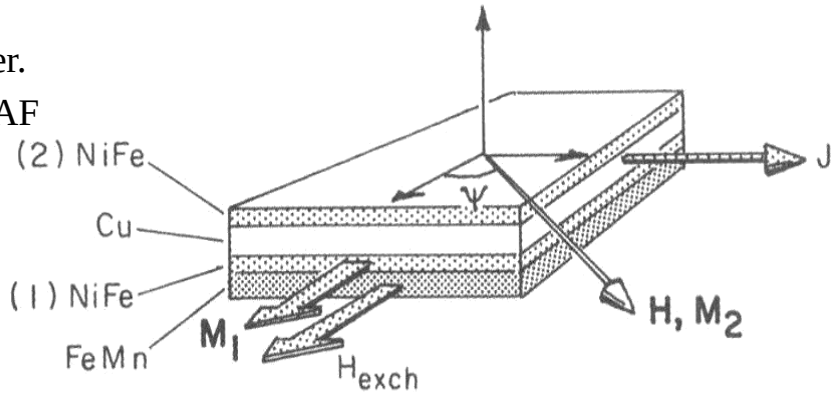

Fig 15.33 Typical composite film structure for spin valve

(4) Magnetoresistance

Ferromagnetic Materials

- **Applications : Spin Valves (continued)**

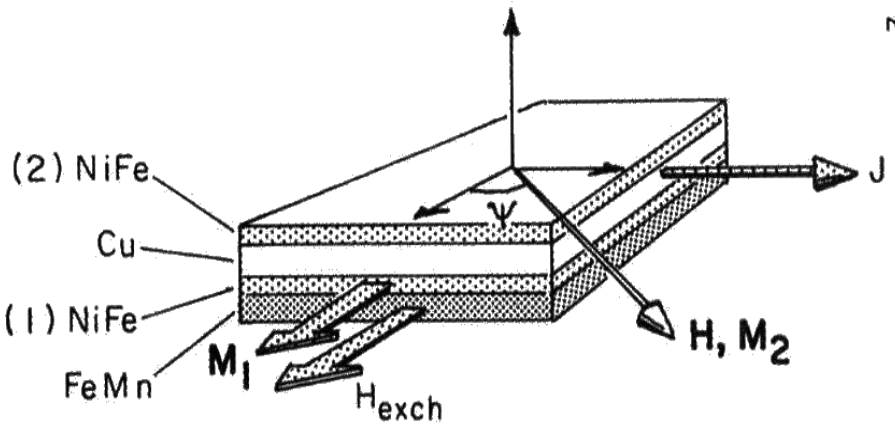

Fig 15.33 Typical composite film structure for spin valve

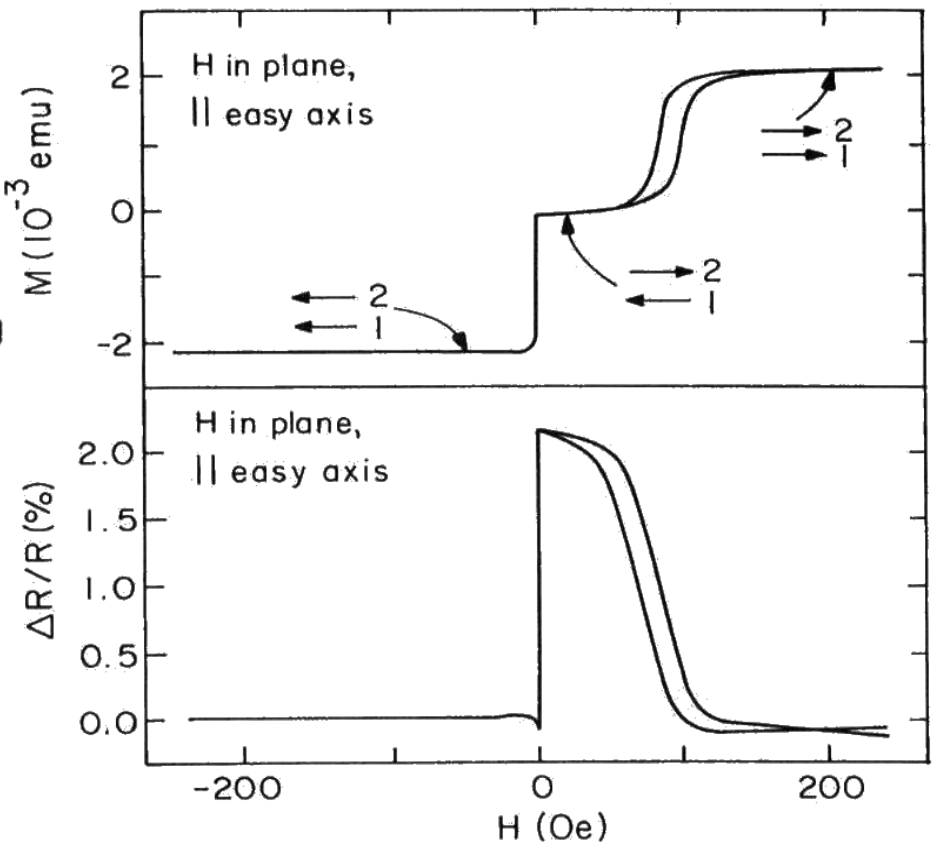

Fig 15.34 Magnetization and relative R change for Si/(NiFe 150Å)/(Cu 26Å)/(NiFe 150Å)/(FeMn 100Å)/(Ag 20Å) J // the easy axis determined by FeMn

(4) Magnetoresistance

Ferromagnetic Materials

▶ **Applications : Spin Valves (continued)**

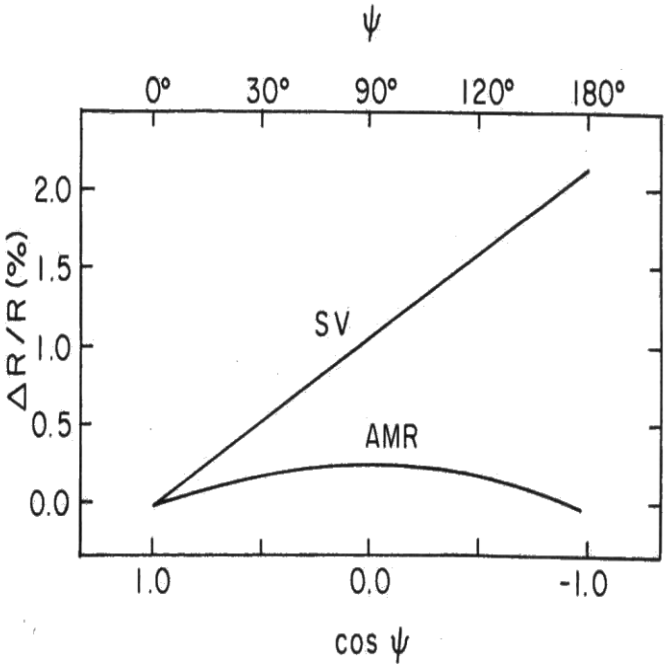

Figure 15.35 Variation of spin valve (SV) resistance and anisotropic magnetoresistance (AMR) with the cosine of the angle between M_1 and M_2. (Dieny et al. 1991).

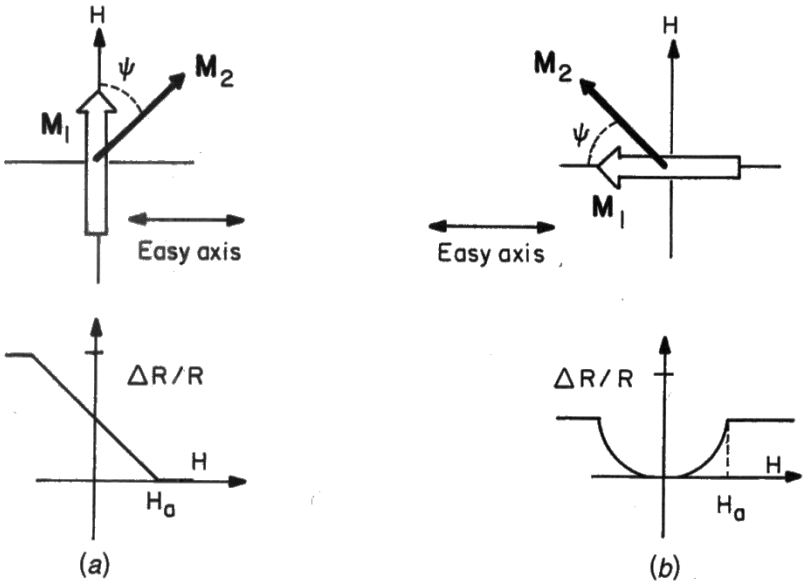

Figure 15.36 (*a*) Hard-axis magnetization process and MR for easy axis perpendicular to the reference magnetization direction (open arrow) in a spin valve structure; (*b*) hard-axis magnetization process and MR for spin valve with easy axis parallel to the reference magnetization direction.

Eq. (15.33) in O'handley

$$\frac{\Delta R}{R} = \frac{\Delta \rho}{\rho}\left(\frac{1 - H/H_a}{2}\right)$$

Eq. (15.34) in O'handley

$$\frac{\Delta R}{R} = \frac{\Delta \rho}{\rho}\left(\frac{1 - \sqrt{1-(H/H_a)^2}}{2}\right)$$

(4) Magnetoresistance

▶ Applications

Spin Switch (Johnson and Silsbee, 1988)

- A magnetic film device similar to a spin valve : Two thin magnetic layers sandwiching a nonmagnetic metal layer.
  The current in a spin switch passes through the thin direction of the sandwich (spin injection)
- The concept of spin injection (see Fig. 15.37) for a ferromagnetic-paramagnetic bilayer
- Three-layer sandwich of spin switch (see Fig. 15.38)
  A weak ferromagnetic layer (F_1)/ Intermediate paramagnetic layer (P)
  : thickness d / A strong ferromagnetic layer (F_2)
  F_1 & F_2 are not exchanged coupled through P.
  $d < \delta_s = (2D_sT_2)^{1/2}$ where δ_s is the avg. distance that an electron could travel without loss of its original spin direction, D_s is the spin diffusion constant, and T_2 is transverse relaxation time
- δ_s (spin diffusion legnth) exceeds the mean free path of charge transport by a few orders of magnitude (*i.e.*, spin-altering collisions occur much less frequently than od momentum-altering collisions)
- The flow of magnetic moment I_M into P by spin transport:
  $\boldsymbol{I_M = \eta I\mu_B/e,\ \eta = (J^{\uparrow} - J^{\downarrow})/(J^{\uparrow} + J^{\downarrow})}$ (η : a current polarization factor)
- The nonequilibrium magnetization buildup M_P in P
  $\boldsymbol{M_P = I_M T_2/Ad}$ (volume of P)

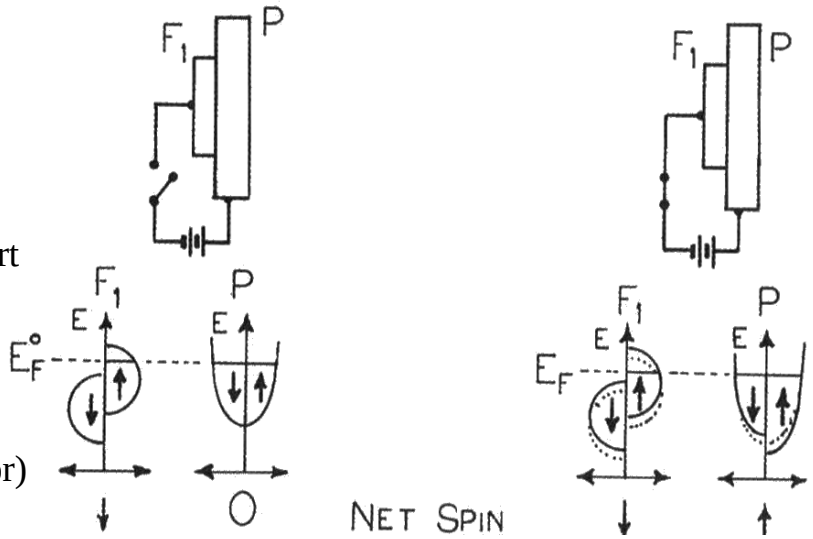

Fig 15.37 Schematic of a spin injection bilayer and state density representations explaining its operation

(4) Magnetoresistance

▶ Applications Spin Switch (continued)

How can the spin-up electrons that make up M_P be drained from P or trapped there? Ans. F_1-P-F_2 three-layer sandwich

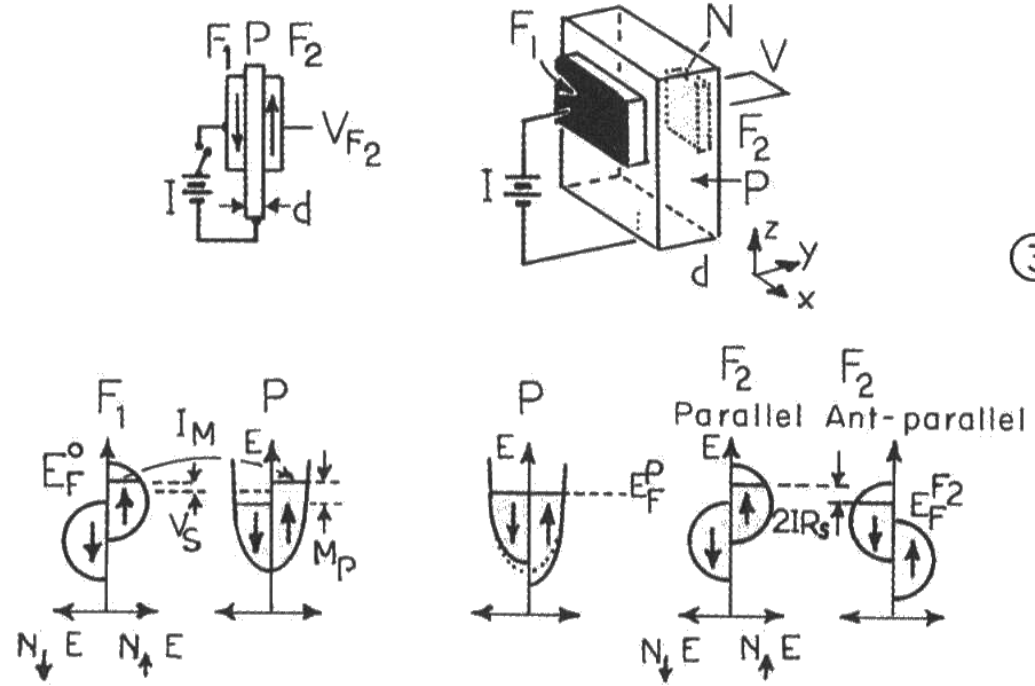

Fig 15.38 Schematic of three-layer sandwich of spin switch

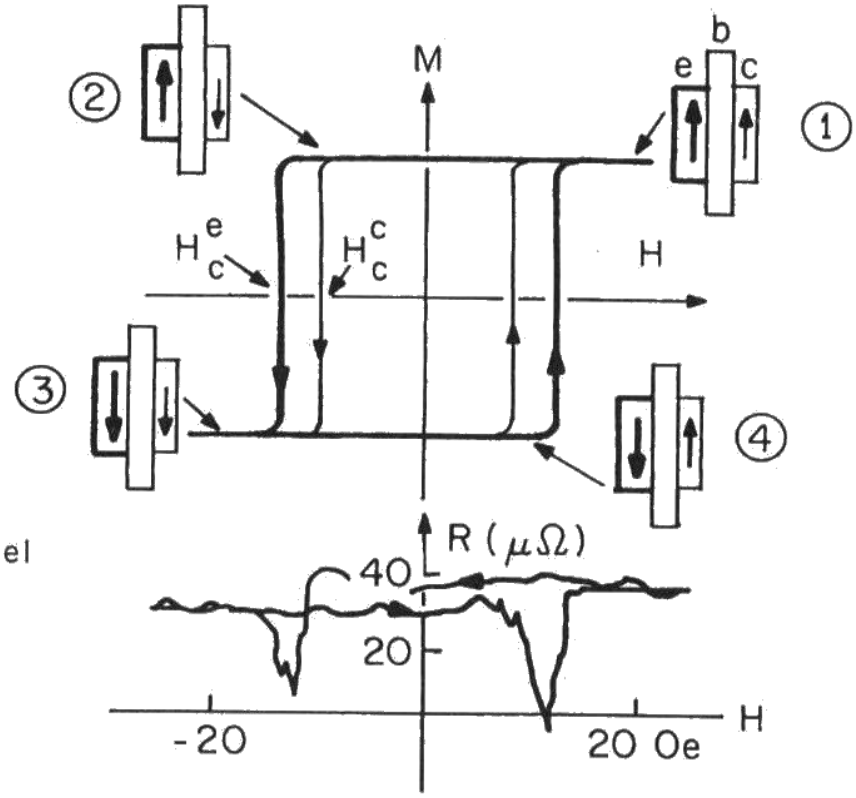

Fig 15.39 Top: *M-H* loop of the emitter (e) and collector (c) and configuration of their magnetization at different points relative to the loops. Bottom: the impedance versus field *H*

(4) Magnetoresistance

▶ Applications

Spin tunneling junctions

- In spin tunnel junction, the nonmagnetic spacer layer is an insulator.
- F-I-F Tunneling (1st by Julliere et al., (1975)) for Fe/Ge/Co
- A magnetoconductance ratio, $\triangle G/G = (G_F - G_A)/G = 2P_1P_2/(1+P_1P_2)$

  P_1, P_2: spin polarizations of the two ferromagnetic electrodes.
- FeCo-Al_2O_3-Co junction: Moodera *et al.* (1996) (see Fig. 15. 43)
- CoFe-MgO(001)-CoFe TMR=220% (2004) S.S Parkin
- Temperature dependence: Primarily due to the decrease in surface magnetization of the electrodes with increasing temperature. (see Fig. 15.44)

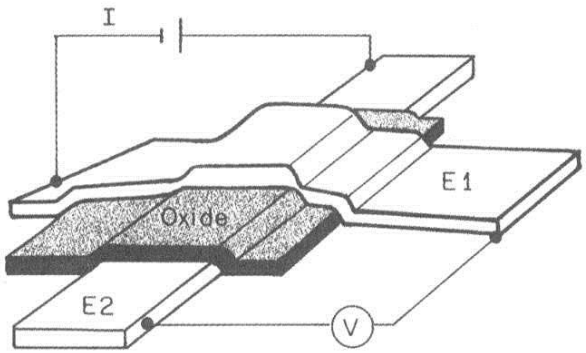

Fig 15.40 Schematic of a patterned tunnel junction. E1 electrode deposited over the oxide on E2 electrode.

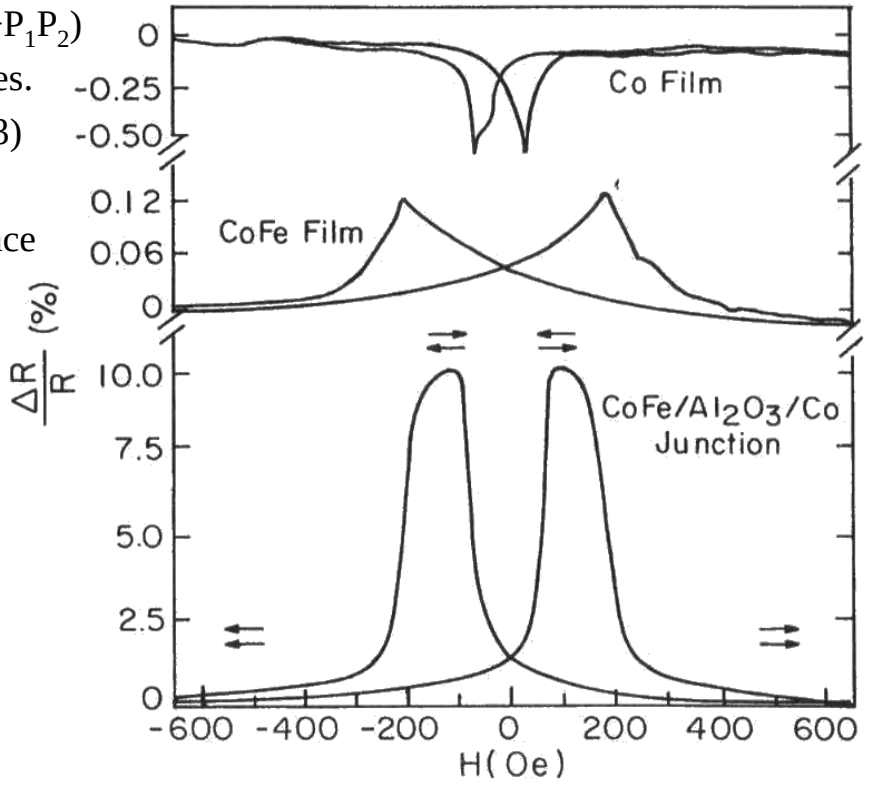

Fig 15.43 Top: Anisotropic MR in each individual CoFe and Co electrode. Bottom: Junction MR in CoFe-Al_2O_3-Co spin tunnel junction vs H.

(4) Magnetoresistance

▶ Summary

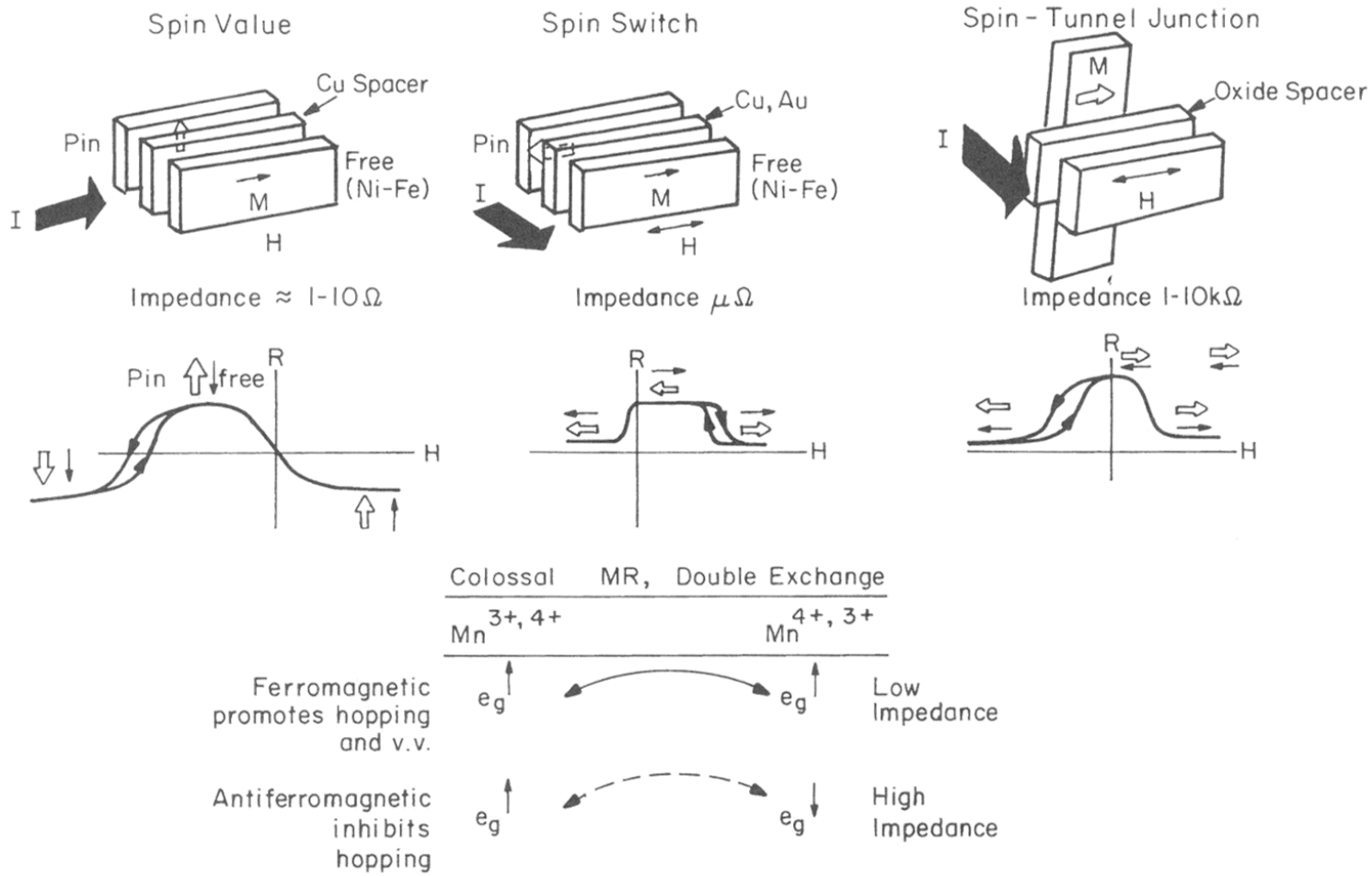

Fig 15.49 summary diagram comparing the structure, current directions, and magnetizations)pinned layers indicated by open arrows), above, as well as galvanomagnetic characteristics of spin valves, spin switches, and tunnel junctions, middle. Below, the essence of the mechanism of colossal magnetoresistance is represented with the spin directions of hopping sites indicated.